

Defect-induced luminescence in high-resistivity high-purity undoped CdTe crystals

This article has been downloaded from IOPscience. Please scroll down to see the full text article.

2002 J. Phys.: Condens. Matter 14 13203

(<http://iopscience.iop.org/0953-8984/14/48/369>)

View [the table of contents for this issue](#), or go to the [journal homepage](#) for more

Download details:

IP Address: 171.66.16.97

The article was downloaded on 18/05/2010 at 19:16

Please note that [terms and conditions apply](#).

Defect-induced luminescence in high-resistivity high-purity undoped CdTe crystals

N Armani, C Ferrari, G Salviati, F Bissoli, M Zha, A Zappettini and L Zanotti

CNR—IMEM Institute, Parco Area delle Scienze, 37/A 43010 Fontanini, Parma, Italy

E-mail: narmani@maspec.bo.cnr.it

Received 27 September 2002

Published 22 November 2002

Online at stacks.iop.org/JPhysCM/14/13203

Abstract

This work focuses on the influence of stoichiometry deviation (Cd/Te excess in the crystal) on the type and density of crystalline defects. In particular, we report a study on the evaluation of extended defects and precipitates, carried out by specific preferential etching, high-resolution x-ray diffraction, double-crystal x-ray topography and cathodoluminescence (CL) analyses. A remarkable difference between the crystals grown from the vapour phase and from the melt has been found. Dislocations were found to arrange in cellular structures 2–300 μm in diameter while precipitates were homogeneously distributed on the growth plane. The CL spectra show an intense near-band-edge emission through the whole range of temperatures and two large emission bands centred at 1.2 and 1.4 eV. It has been observed that the luminescence intensity of the 1.4 eV band increases close to crystal defects and simultaneously the near-band-edge intensity decreases. The disappearance of this emission both in the CL spectra and in the CL images on increasing the temperature up to 300 K suggests a donor–acceptor pair nature for the transition involved.

1. Introduction

Cadmium telluride is a technologically important compound semiconductor with a range of applications which require high-quality and defect-free substrates. CdTe also has high electro-optic coefficients and a significant non-linear response to two-photon absorption in the near infrared making it a contender for use in non-linear optical devices. CdTe and CdZnTe semiconductor gamma detectors have been produced traditionally from crystals grown by the travelling heater method [1], or by the high-pressure Bridgman (BG) method [2].

A high-mobility-lifetime product requires a low concentration of defects in the crystal, including two- and three-dimensional structural defects such as grain boundaries and Cd–Te inclusions or precipitates. Usually crystalline defects resulting in deformation of the lattice are obstacles to the carrier flow and behave as non-radiative recombination centres. In contrast,

the point defects (native or impurity) [3], present in high concentration in Cd-based II–VI compounds, lead to the formation of energy levels in the gap which influence the electrical and optical properties of the material [4, 5].

In this paper we report a study on the nature and distribution of defects found in CdTe crystals grown by physical vapour transport (PVT) and modified BG techniques. The crystal quality of the specimens is checked by the high-resolution x-ray diffraction technique (HRXRD) and by x-ray topography, which provides information on the defects responsible for the distortion of the crystal lattice. Furthermore, the nature and the spatial distribution of these defects are studied by means of the acquisition of cathodoluminescence (CL) micrographs as well as CL spectra, possible thanks to the high lateral resolution of this technique.

2. Crystal growth and experimental procedure

The crystals studied were grown by the PVT and vertical BG techniques starting from heat-treated [6] polycrystalline CdTe, previously synthesized from 7N purity Cd and Te [7].

2.1. The vapour phase transport technique

A horizontal configuration has been adopted. Separated heating controllers (Eurotherm 818) controlled the three zones of the furnace with a temperature fluctuation within $\pm 0.2^\circ\text{C}$. Due to the poor heat conductivity of CdTe, the applied temperature profile was set to have a steep temperature gradient at the crystallization end. The closed quartz ampoule was provided with a short capillary at the crystallization end. The capillary was part of the core of a quartz bar (10 cm long and 1 cm in diameter), coaxial with the ampoule, which further favoured heat release. The effect of the attached bar was evidenced by the convex shape of the growing interface, on which there appeared a number of facets. The furnace was designed so as to move with respect to the fixed growth ampoule with a constant speed in the range from 1 to 10 mm/day. A 3 mm/day moving speed was applied in these growth experiments, which yielded crystals up to 27 mm in diameter and several centimetres in length. The post-growth cooling rates were of the order of $20\text{--}40^\circ\text{C h}^{-1}$.

2.2. The vertical Bridgman technique

The BG technique was carried out with a charge (70 g). Boric oxide (B_2O_3) encapsulation effectively reduced the losses of components, especially cadmium. A pressure of a few atmospheres of inert gas (usually nitrogen) was applied to reinforce the encapsulation effect. The ampoule was rotated at 15 rpm while being moved downwards at a speed of 2 mm h^{-1} . The post-growth cooling rates were of the order of $20\text{--}40^\circ\text{C h}^{-1}$. Crystal ingots made of large single grains were grown in about 36 h.

3. Structural and electrical characterization

The resistivity of the crystals was measured by Van der Pauw measurements at room temperature. The structural characterization was performed by means of HRXRD. A Philips diffractometer with a four-reflection (220) Ge monochromator was used to acquire the $\omega\text{--}2\theta$ rocking curves. The topographic images were obtained with a double-crystal diffractometer using a 620 asymmetric Ge monochromator and the 422 reflection. In this work we report on

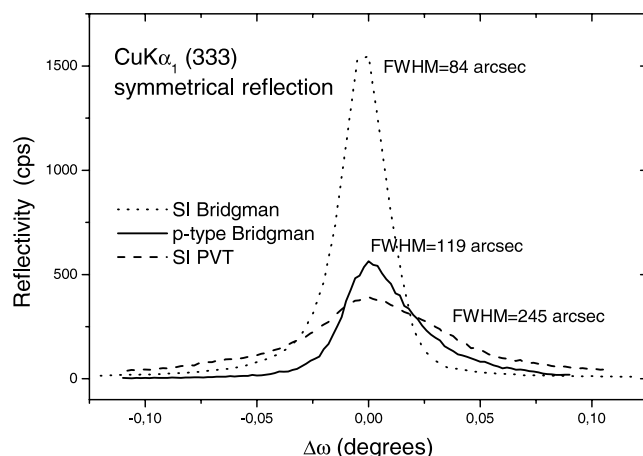


Figure 1. HRXRD rocking curves for the Cu $K\alpha_1$ (333) symmetrical reflection of a PVT grown crystal, a high-resistivity BG grown crystal and a p-type BG grown sample.

high-resistivity (10^7 – 10^8 Ω cm) PVT and BG grown samples and low-resistivity BG grown samples.

The HRXRD rocking curves for the (333) symmetrical reflection are shown in figure 1. The curves relating to the PVT grown crystal are characterized by a low intensity and a large FWHM with respect to the BG grown samples. The broadening of the PVT grown crystal HRXRD profiles is due to the presence of unstrained subgrains. Due to the difference between the monochromator and sample Bragg angles, the configuration results are slightly dispersed. In this configuration the typical orientation contrast vanishes and the contrast in the pictures is mainly due to the presence of defects. In figure 2 an x-ray topograph of a p-type BG grown crystal evidences the presence of precipitates together with dislocations emerging at the surface. The image demonstrates a single crystal with low-angle grain boundaries present with angles in the range of a few tens of seconds of arc.

4. Cathodoluminescence analyses

The optical analyses were performed by a Gatan monoCL system mounted on a Cambridge 360 scanning electron microscope. The spectra as well the panchromatic and monochromatic images were acquired using a dispersion system, equipped with two diffraction gratings and a system composed of a photomultiplier and a Ge detector. This experimental set-up provides a spectral resolution of 1 \AA and a detectable 750–1600 nm (0.9–1.6 eV) wavelength range, covering the whole CdTe spectrum.

The luminescence properties of the crystals were studied by means of the SEM–CL technique; the electron beam energy was chosen in order to reach a penetration depth of several microns (up to 4.2 μm) to avoid any influence of the surface recombination on the CL signal. In figure 3 the low-temperature CL spectra of the samples investigated by the x-ray diffraction method are shown. The 77 K curves present an intense NBE emission, made up of the excitonic transitions [8] centred at 1.59 eV and two large bands centred at 1.2 and 1.4 eV respectively. The band at 1.4 eV is not observed for p-type samples and its energy position shifts toward high energy for semi-insulating samples with respect to the n-type ones. By acquiring CL spectra at $T = 5$ K, as shown in the inset of figure 3, the emission band of the SI

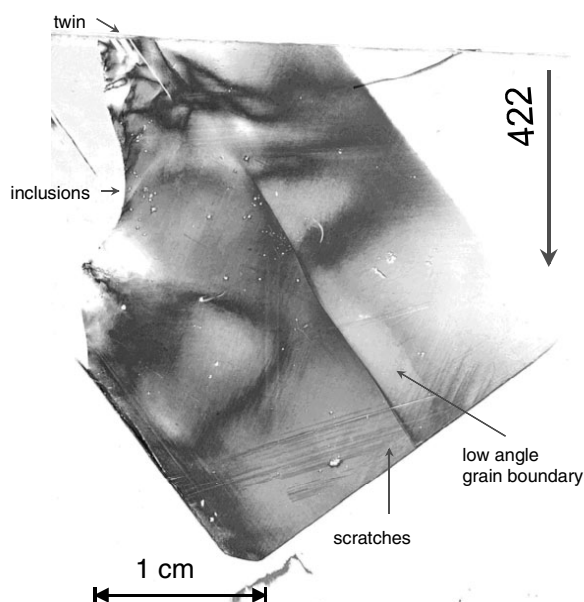


Figure 2. A double-crystal topographic image of the Cu $K\alpha$ (422) asymmetrical reflection of the semi-insulating sample.

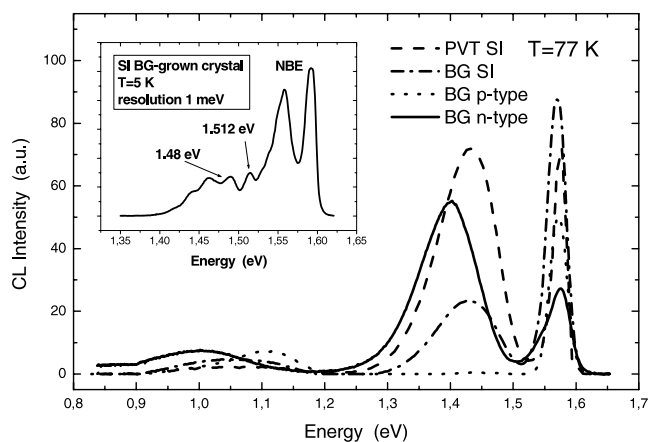


Figure 3. CL spectra at 77 K of the crystals previously analysed by means of HRXRD. In the inset the 1.4 eV band for a SI crystal at 5 K is shown.

crystals can be resolved by deconvolution into Gaussian curves into two different emissions. The CL bands are centred at 1.48 and 1.512 eV and can be attributed to native defect complexes and to impurities [9–11] respectively. The native defects related to the 1.2 eV band have been discussed elsewhere [12].

The structural deformations produced by the defects observed in the topographic analyses can be correlated with the luminescence properties evidenced in the CL images. In figure 4 a monochromatic CL image taken at the NBE emission energy (1.59 eV) of the semi-insulating crystal of figure 2 is shown. The picture shows dark regions several microns in diameter, denoted as non-radiative recombination centres. From their dimension it is possible to

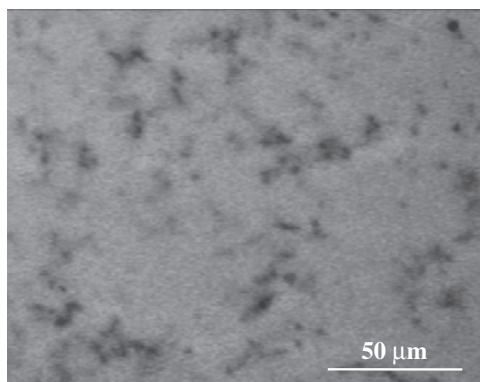


Figure 4. A low-temperature (77 K) CL monochromatic image of the semi-insulating crystal of figure 2 at the NBE emission energy (1.59 eV).

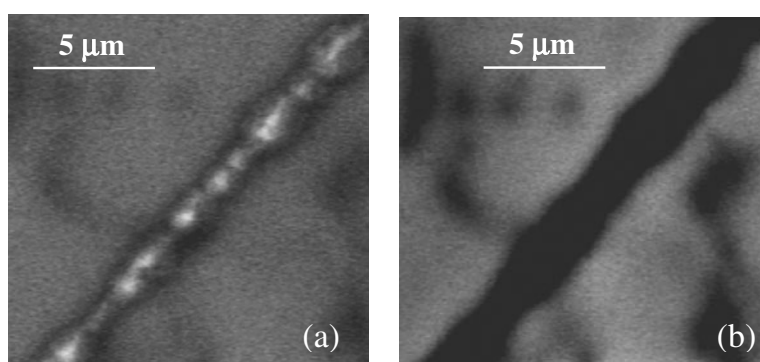


Figure 5. CL monochromatic images of the semi-insulating crystal acquired in a region with a large density of crystal defects, (a) at 1.4 eV, (b) at 1.59 eV, the NBE emission energy.

distinguish between inclusions, 10–15 μm , and precipitates, 1–2 μm , both consisting of non-luminescent metallic Cd–Te compounds. The dislocations, which are difficult to distinguish from the precipitates, act also as non-radiative recombination centres. By comparing the topographic and monoCL images, the natures of the different defects can be studied. The inclusions clearly visible in both analyses are distributed randomly in the crystal, but their density is substantially larger in the p-type material. In SI crystals a large number of smaller defects arranged in cellular structures with dimensions of 100–200 μm can be observed.

Preferential etching on SI BG grown samples evidenced a series of crystallographic defects several microns in length. MonoCL images of such defects are shown in figure 5. While the image acquired at the NBE emission energy reveals a totally dark area arising from inside the defect structure, the 1.4 eV image shows a bright area originating inside the defect. Spectroscopic CL spot-mode investigations, performed focusing the electron beam inside and outside the defects, are shown in figure 6. The curves acquired inside the defect reveal a strong decrease of the NBE emission intensity, while the intensity of the 1.4 eV band remains almost constant. The same type of analysis was performed also for inside and outside the dark regions visible in the monoCL images of figure 4; in this case the spectra obtained showed a constant decrease of all the CL emission band intensities, revealing a non-radiative recombination nature for the defects involved.

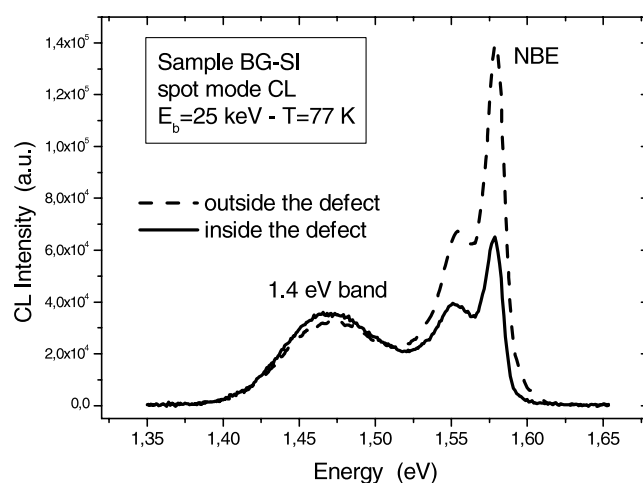


Figure 6. Spot-mode CL spectra, at 77 K, with the electron beam focused inside (solid curve) and outside (dashed curve) the crystalline defects shown in figures 5(a) and (b).

Similar optical behaviour of the dislocations in CdTe crystals has also been found in intentionally indented samples [13] and the energy of the luminescence band, named ‘Y luminescence’, is found at 1.47 eV [14]. Temperature-dependent measurements which revealed the vanishing of the CL intensity at temperature above 150 K suggest a donor–acceptor pair nature lying at the origin of the 1.4 eV band. The gathering at the defects of impurities incorporated in the crystals during BG growth could also be responsible for such emission.

5. Conclusions

The structural and optical properties of CdTe high-purity crystals have been studied by means of HRXRD, x-ray topography and CL techniques. The measurements show that the BG grown samples have the better crystalline quality—in particular the semi-insulating crystals with respect to the p- and n-type ones. The topographies and the monoCL images give information on the densities of the defects, inclusions, precipitates and dislocations. BG grown specimens $2 \times 2 \text{ cm}^2$ in size are single crystals with a dislocation density in the range 10^5 cm^{-2} . Microscopic CL investigations, performed on semi-insulating materials, reveal a radiative recombination nature for defects observed after preferential etching. The emission band is centred at 1.4 eV and is attributed to the gathering at the dislocations of impurities.

References

- [1] Song S H, Wang J and Isshiki M 2002 *J. Cryst. Growth* **236** 165
- [2] Korbutyak D V, Krylyuk S G, Tkachuk P M, Tkachuk V I, Korbutyak N D and Raransky M D 1999 *J. Cryst. Growth* **197** 659
- [3] Berding M A 1999 *Phys. Rev. B* **60** 8943
- [4] Seto S, Tanaka A, Takeda F and Matsuura K 1994 *J. Cryst. Growth* **138** 346
- [5] Guergouri K, Brihi N and Triboulet R 2000 *J. Cryst. Growth* **209** 709
- [6] Zha M, Bissoli F, Zappettini A, Zuccalli G, Zanotti L and Paorici C 2002 *J. Cryst. Growth* **237–239** 1720
- [7] Zappettini A, Görög T, Zha M, Zanotti L, Zuccalli G and Paorici C 2000 *J. Cryst. Growth* **214–215** 14
- [8] Shin H Y and Sun C Y 1998 *Mater. Sci. Eng. B* **52** 78

-
- [9] Stadler W, Hoffmann D M, Alt H C, Muschik T, Meyer B K, Weigel E, Müller-Vogt G, Salk M, Rupp E and Benz K W 1992 *Phys. Rev. B* **45** 10619
 - [10] Castaldini A, Cavallini A, Fraboni B, Fernández P and Piqueras J 1998 *J. Appl. Phys.* **83** 2121
 - [11] Soares M J and Carmo e M C 1997 *J. Lumin.* **72–74** 719
 - [12] Armani N, Ferrari C, Salviati G, Bissoli F, Zha M and Zanotti L 2002 *Mater. Sci. Eng. B* **91–92** 353
 - [13] Schreiber J, Höring L, Uniewski H, Hildebrandt S and Leipner H S 1999 *Phys. Status Solidi a* **171** 89
 - [14] Schreiber J, Hilpert U, Höring L, Worschech L and Ramsteiner M 1999 *Inst. Phys. Conf. Ser.* **169** 561